Heat Capacities and Derived Thermodynamic Functions of *n*-Nonadecane and *n*-Eicosane between 10 K and 390 K

J. Cees. van Miltenburg,*,† Harry A. J. Oonk,† and Valerie Metivaud‡

Chemical Thermodynamics Group, Utrecht University, Padualaan 8, NL-3584 CH Utrecht, The Netherlands, and Centre de Physique Moléculaire Optique et Herzienne, URA 283 au CNRS, Université Bordeaux I, 351, Cours de la Libération, F-33405 Talence Cedex, France

Heat capacity measurements were made on *n*-nonadecane and *n*-eicosane from 10 K to 390 K with an adiabatic calorimeter. These measurements were used to calculate the entropy and the enthalpy relative to 0 K. The sum of the enthalpy of the solid−solid transition and of melting of *n*-nonadecane is 62659 ± 20 J·mol⁻¹ at the triple point, 305.00 K. The enthalpy of melting of *n*-eicosane was calculated to be 69922 ± 100 J·mol⁻¹ at the triple point, 309.65 K. The entropies were extrapolated from the liquid phase just above the melting point to 298.15 K and found to be respectively 715.8 and 748.1 J·K⁻¹·mol⁻¹. The crystallization behavior of both compounds is discussed.

Introduction

The low-temperature thermodynamic functions of the *n*-alkanes have been measured by several groups between the 1930s and the 1960s. The research on the hydrocarbons was encouraged by the oil industry. The complete set of *n*-alkanes, ranging from ethane to *n*-octadecane, was measured (Parks et al., 1930; Huffman et al., 1937; Parks et al., 1937; Stull, 1937; Witt and Kemp, 1937; Kemp and Egan, 1938; Aston and Messerly, 1940; Parks et al., 1949; Finke et al., 1954; Schaerer et al., 1954; Messerly et al., 1967). The availability of such a set of data on a homologous series of compounds offers the possibility to look for relations such as group contributions and dependence of thermodynamic properties on the number of carbon atoms in the linear molecule. One important property, the absolute entropy $S°(T)$, is calculated by integrating the measured heat capacities divided by the temperature between 0 K and the stated temperature. Messerly et al. (1967) published a critical evaluation of the available entropy values at 298.15 K and proposed an improved quadratic fit for the *n*-alkanes ranging between *n*-pentane and *n*-octadecane. It is however always risky to extrapolate fitted data out of the measured range, and one of the objects of this study is to see if this extrapolation is warranted.

More recently, there is renewed interest in the *n*-alkane series, especially for the higher members of the series, as shown by the literature (Barbillon et al., 1991; Mondieig et al., 1997; Oonk et al., 1998). Much work has been done on the study of phase diagrams formed by binary mixtures of neighbors and next-nearest neighbors of the *n*-alkanes. We work on these kinds of systems, together with other research groups united in the REALM (Réseau Européen sur les Alliages Moléculaires). The properties of the *n*-alkanes seem to make them good candidates for the storage of thermal energy. In this application, the cooling behavior of the compounds is very important. One of the requirements is little or no subcooling in the bulk phase. That is

the reason that we report cooling curves made by adiabatic calorimetry.

Experimental Section

C₁₉H₄₀ was purchased from Fluka Chemica, with an estimated purity of better than 99%. C₂₀H₄₂ came from Aldrich with a stated purity of 99%. Measurements were performed on 4.20 and 3.65 g, respectively. The hydrocarbons were sealed in a gold-plated copper calorimeter vessel. After a short evacuation, about 1000 Pa of helium gas was added in order to improve heat conduction. The calorimeter used (laboratory-design indication CAL VII) was built as a copy of CALV, which has been described before (Miltenburg et al., 1987). The temperature calibration of the platinum-resistance thermometer used was corrected to the ITS-90 temperature scale (Preston-Thomas, 1990). The heat capacities are estimated from measurements on *n*-heptane and synthetic sapphire to deviate within ±0.02% and have an accuracy of ±0.2%.

Often, the thermal history of the sample has an influence on the heat capacity measurements. With these compounds, however, no differences were found between the different series at the same temperatures. For each compound, two cooling curves, including the crystallization, were measured. In these cases an amount of about 5000 Pa of helium was admitted into the separate vacuum chamber of the calorimeter which surrounds the vessel and the shields. This resulted in a cooling rate, outside the crystallization region, of about 1 deg·min⁻¹.

Results and Discussion

Our experimental data series are given in chronological order in Tables 1 and 2. The derived thermodynamic properties $H°(T) − H°(0)$ and $S°(T)$ are given in Tables 3 and 4. The values at 10 K were calculated using the low-temperature limit of the Debye equation $C_p = \alpha T^3$. Our measurements do not extend to sufficient low temperatures for constancy of C_p/T^3 to be reached. The fitted values of C_p at 10 K were used to estimate α. The values of α used for C₁₉H₄₀ and C₂₀H₄₂ are respectively 0.0033 and 0.0032 J·K⁻⁴·mol⁻¹. An accuracy in these α values of about 10%

* Corresponding author. Fax: +31 302533946. E-mail: miltenb@chem.uu.nl.
† Utrecht University.
‡ Université Bordeaux.

Table 1. Experimental Data Series of n-Nonadecane

T/K	$C_p/\mathrm{J \cdot K^{-1} \cdot mol^{-1}}$	T/K	$C_p/\mathrm{J \cdot K^{-1} \cdot mol^{-1}}$	T/K	$C_p/\mathrm{J \cdot K^{-1} \cdot mol^{-1}}$	T/K	$C_p/\mathrm{J \cdot K^{-1} \cdot mol^{-1}}$	T/K	$C_p/\mathrm{J \cdot K^{-1} \cdot mol^{-1}}$
Series 1		262.59	436.50	20.70	21.33	111.79	224.10	292.81	594.49
272.37	460.49	264.56	441.09	22.94	26.55	114.68	228.10	294.67	1470
273.54	464.72	266.54	446.13	25.28	32.30	117.58	232.06	295.44	19482
275.48	471.02	268.51	451.03	27.73	38.94	120.48	236.00	295.54	54110
277.41	477.53	270.47	456.23	30.26	46.00	123.38	239.82	295.59	56664
279.33	484.42	272.42	461.73	32.88	53.20	126.29	243.60	295.71	15519
281.23	492.21	274.36	467.73	Series 4		129.20	247.32	296.65	1091
283.12	500.63	276.30	474.27	8.30	2.18	132.12	250.99	298.34	1077.10
284.99	510.14	278.22	480.90	9.91	3.30	135.04	254.54	299.96	1239.71
286.85	521.16	280.13	488.03	11.48	4.27	137.96	258.13	301.41	1523.20
288.69	534.23	282.03	495.72	13.38	7.02	140.89	261.67	302.63	2118.56
290.51	551.52	283.91	504.76	15.17	9.92	143.82	265.20	303.52	3559.78
292.29	580.13	285.78	514.52	17.00	13.50	146.75	268.67	304.08	6831.39
293.99	672.32	287.63	526.15	19.06	17.51	149.69	272.13	304.39	12638
295.06	3939.21	289.46	540.95	21.26	22.39	152.63	275.62	304.57	21564
295.34	31223	291.26	560.92	23.54	27.83	155.57	279.12	304.68	35268
295.41	35430	293.02	601.69	25.92	33.80	158.51	282.59	304.75	52972
295.47	34967	294.54	1032.76	28.39	40.56	161.46	286.13	304.80	77663
295.54	28741	295.32	8306	30.94	47.31	164.40	289.86	304.83	107255
295.65	15708	295.48	31139	Series 5		167.34	293.58	304.86	149733
296.30	1232.76	295.54	49914	6.86	1.20	170.29	297.18	304.88	183709
297.55	1018.02	295.58	52253	8.32	1.82	173.24	300.64	304.89	179657
298.83	1109.81	295.64	34889	9.94	3.33	176.20	304.19	304.91	240230
300.04	1238.59	295.88	4605	11.82	4.44	179.16	307.77	304.92	428085
301.15	1434.40	296.77	978.98	13.66	7.66	182.11	311.47	304.92	398384
302.14	1765.82	298.09	1056.36	15.40	10.56	185.06	315.02	305.02	16704
302.97	2401.28	299.34	1162.64	17.29	13.95	188.01	318.69	306.23	631.94
303.59	3705.12	300.50	1316.73	19.44	18.37	190.97	322.47	308.50	605.32
304.01	6210.22	301.56	1562.29	21.64	23.26	193.93	326.28	310.79	606.70
304.28	10267	302.48	1992.93	23.94	28.76	196.88	330.13	313.08	608.10
304.45	15886	303.22	2830.67	26.34	34.99	199.84	334.06	315.37	609.44
304.57	23239	303.76	4464.64	28.82	41.72	202.80	337.58	317.65	611.12
304.65	33064	304.13	7304.18	31.39	48.58	205.76	341.54	319.93	612.82
304.71	46911	304.36	11659	Series 6		208.72	345.64	321.31	614.51
304.75	61774	304.51	17936	34.07	56.71	211.68	349.76	322.30	615.21
304.79	78606	304.62	26731	36.73	64.52	214.64	353.86	324.15	616.67
304.81	99267	304.69	38298	39.06	71.12	217.59	358.17	326.14	618.26
304.83	119468	304.74	52131	41.33	77.59	220.51	362.41	328.13	619.75
304.85	129501	304.77	69863	43.70	84.42	223.42	366.71	330.12	621.46
304.87	179280	304.80	92456	46.11	91.40	226.31	371.07	332.10	623.17
304.88	215038	304.83	106879	48.55	98.19	229.18	375.36	334.09	624.46
304.89	193478	304.85	130176	51.04	104.82	232.04	379.92	336.08	626.56
304.89	2208807	304.86	191213	53.57	111.57	234.88	384.42	338.07	628.20
304.90	340488	304.87	222384	56.13	118.22	237.70	389.11	340.06	629.48
304.91	179312	304.88	263585	58.72	124.95	240.50	393.85	342.05	630.86
304.93	102804	304.89	302733	61.34	131.48	243.29	398.62	344.04	632.71
305.21	3421	304.90	154872	63.99	137.79	246.06	403.54	346.04	634.75
306.35	604.92	304.91	180533	66.66	144.05	248.81	408.67	348.03	636.51
308.08	606.08	304.93	62277	69.36	150.23	251.55	413.91	350.02	637.99
309.81	606.63	305.54	1227.60	72.08	156.08	254.27	419.20	352.01	639.84
311.53	607.69	306.98	605.52	77.63	167.21	256.98	424.61	354.00	641.78
Series 2		308.71	605.98	80.38	172.60	259.67	430.31	356.00	643.60
241.17	392.60	310.43	606.88	83.15	177.87	262.34	436.13	358.00	645.49
241.60	393.45	312.15	607.87	85.95	183.01	265.00	442.33	359.99	647.38
242.80	396.94	313.86	603.59	88.76	188.03	267.64	448.87	361.99	649.46
244.78	400.59	Series 3		91.60	192.96	270.26	455.85	363.99	651.16
246.76	404.54	7.30	1.61	94.43	197.70	272.86	463.33	365.99	652.92
248.74	408.11	8.65	2.53	97.27	202.30	275.44	471.23	367.98	654.71
250.72	411.95	9.61	3.51	100.08	206.72	278.00	479.88	369.98	656.69
252.70	416.09	11.26	4.41	Series 7		280.54	489.54	371.97	658.52
254.67	419.89	13.06	6.62	102.54	210.57	283.06	500.73	373.97	660.68
256.65	424.01	14.78	9.38	103.87	212.59	285.56	514.07	375.96	662.55
258.63	428.08	16.56	12.70	105.98	215.80	288.02	529.70	377.96	664.85
260.61	432.21	18.54	16.55	108.90	220.02	290.45	551.51	379.96	666.53

is to be expected. Figure 1 displays the α values that were estimated from the C_p(10 K)/1000 values as given by Messerly et al. (1967) for C_5H_{12} to $C_{17}H_{36}$, by us for $C_{19}H_{40}$ and $C_{20}H_{42}$, and by Andon and Martin (1976) for $C_{26}H_{54}$. Despite a large error margin in some of these values, an even−odd effect is clearly visible.

Melting Behavior and Purity Determination for n-Nonadecane. In Figure 2 molar heat capacity data of n-nonadecane are given around the solid−solid transition and the melting event. The molar heat capacity between the transition and the melt temperatures is exceptionally high and is completely reproducible. It does not depend on the thermal history of the sample or the mean heating rate of the interrupted measurements. The effect is much too large to be attributed to a premelting effect. We consider this effect to be a true aspect of this compound. Previously, similar observations have been made for other odd members of the n-paraffin's (Messerly et al., 1967). The effect was attributed to the "rotary state" in the solid phase, in which the linear molecules can rotate along the long axes.

Table 2. Thermodynamic Properties at Selected Temperatures for Nonadecane
($C_{19}H_{40}$) ($M = 268.52$ g·mol^{-1}; $\Phi_m^\circ \stackrel{\text{def}}{=} \Delta_0^T S_m^\circ - \Delta_0^T H_m^\circ / T$)

| T/K	$C_{p,m}^\circ$/ J·K^{-1}·mol^{-1}	ΔS_m°/ J·K^{-1}·mol^{-1}	ΔH_m°/ J·mol^{-1}	Φ_m°/ J·K^{-1}·mol^{-1}
10	3.378	1.087	8.155	0.2718
15	9.894	3.415	38.00	0.8818
20	19.60	7.522	110.52	1.997
25	31.46	13.13	237.30	3.640
30	44.84	20.05	427.98	5.783
35	59.47	28.03	687.90	8.379
40	73.79	36.92	1021	11.38
45	88.20	46.44	1426	14.74
50	102.04	56.46	1902	18.41
55	115.29	66.81	2446	22.34
60	128.20	77.40	3055	26.49
65	140.18	88.14	3726	30.81
70	151.67	98.95	4456	35.29
75	161.98	109.77	5240	39.90
80	171.86	120.54	6075	44.60
85	181.29	131.25	6958	49.39
90	190.20	141.86	7887	54.23
95	198.62	152.38	8859	59.12
100	206.60	162.77	9873	64.04
105	214.31	173.04	10925	68.99
110	221.58	183.18	12015	73.95
120	235.36	203.05	14300	83.88
130	248.33	222.41	16719	93.80
140	260.60	241.26	19264	103.66
150	272.50	259.65	21930	113.45
160	284.35	277.61	24714	123.15
170	296.83	295.23	27620	132.75
180	308.82	312.53	30648	142.26
190	321.23	329.56	33798	151.67
200	334.27	346.36	37075	160.99
210	347.42	362.98	40481	170.21
220	361.66	379.47	44026	179.35
230	376.64	395.87	47717	188.41
240	392.99	412.24	51564	197.39
250	410.93	428.64	55581	206.31
260	431.01	445.14	59789	215.18
270	455.13	461.84	64215	224.01
280	487.38	478.69	68919	232.55
290	547.32	496.68	73933	241.73
305[b]	545.4[a]	524.3[a]	82281[a]	252.77
305[c]	602.12	729.18	144276	253.07
310	606.76	739.33	147290	264.20
320	613.31	758.70	153392	279.35
330	621.22	777.71	159568	294.17
340	629.52	796.38	165821	308.67
350	638.20	814.74	172158	322.86
360	647.28	832.84	178584	336.77
370	657.77	850.79	185104	350.51
380	666.68	868.26	191725	363.72

[a] Extrapolated from the solid before the transition. [b] Solid. [c] Liquid

It does however differ from the well-known solid−solid transition into a plastic crystalline phase as in the case of carbon tetrachloride. In those kinds of substances, the heat capacity between the rotation transition and the melting point does not reach such high values, nor does it increase that much with temperature.

For *n*-nonadecane, the anomalously high values of the heat capacity between the transition and the melting point make it impossible to separate the two enthalpic effects. We therefore give in Table 5 the total heat effect, including the transition and the melting. For the calculation the heat capacity of the solid was fitted between 200 K and 260 K to the quadratic function

C_p(solid 200 K to 260 K) =

$$\{458.46 - 2.32824T + 0.008564T^2\} \quad (1)$$

where C_p is in J·K^{-1}·mol^{-1} and T is temperature in K.
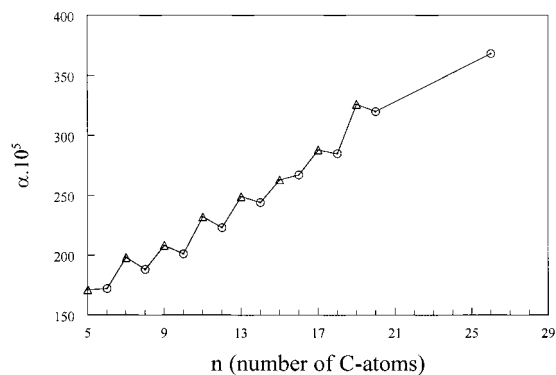
Figure 1. Even−odd effect at 10 K. The molar heat capacity was assumed to fit $C_p = \alpha T^3$ between 0 K and 10 K.
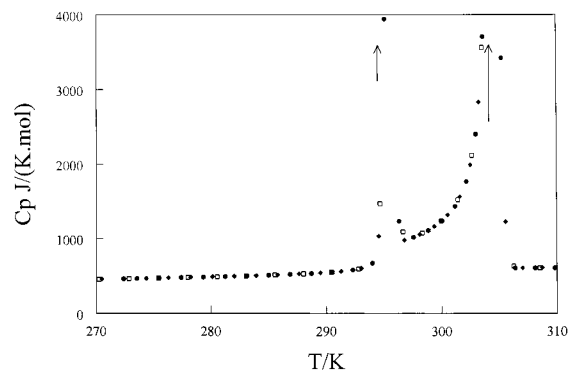
Figure 2. Molar heat capacities of *n*-nonadecane; different measuring series are given: (●) series 1; (◆) series 2; (□) series 7 and 8.

Equation 1 was used as the baseline, and no iterative calculation was applied. The end-point of the melting process was calculated in the usual way, that is, by plotting the melted fraction against the equilibrium temperature. For this calculation the heat capacity data of the rotary phase were fitted between 297 K and 301 K. The plot of the reciprocal of the melted fraction against temperature was straight, indicating that the choice of baseline was justified. The resulting triple point was 305.00 K. The purity calculated was 99.54%. The molar heat capacity data of the liquid phase were fitted to a second-order polynomial equation:

C_p(liquid 305 K to 390 K) =

$$\{638.14 - 0.88814T + 0.002537T^2\} \quad (2)$$

where C_p is in J·K^{-1}·mol^{-1} and T is temperature in K.

The maximum deviation of this fit from the experimental data is 0.15%.

Melting Behavior of n-Eicosane. *n*-Eicosane does not show a solid−solid-phase transition during heating. The results of three melting experiments are given in Table 6. Schaerer and Busso (1954) reported an enthalpy of fusion of 69875 J·mol^{-1} and a melting temperature of 309.7 K. Claudy and Létoffe (1991) found 66935 J·mol^{-1} and a melting temperature of 310.0 K. The data are all within the combined error margins.

The heat capacity data of the liquid were fitted to the following polynomial function:

C_p(liquid 310 K to 390 K) =

$$\{581.23 - 0.38942T + 0.001852T^2\} \quad (3)$$

where C_p is in J·K^{-1}·mol^{-1} and T is temperature in K.

Table 3. Experimental Data Series for *n*-Eicosane

T/K	C_p/J·K^{-1}·mol^{-1}	T/K	C_p/J·K^{-1}·mol^{-1}	T/K	C_p/J·K^{-1}·mol^{-1}	T/K	C_p/J·K^{-1}·mol^{-1}	T/K	C_p/J·K^{-1}·mol^{-1}
Series 1		309.56	84757	40.22	77.60	193.99	336.92	309.59	229893
297.46	529.43	309.59	192528	42.54	84.66	196.41	339.99	309.60	365175
298.64	532.41	309.63	4046399	44.92	91.60	198.82	343.04	309.61	405579
300.60	542.76	309.64	380825	47.34	98.62	201.22	346.41	309.62	442195
302.53	556.77	309.95	3754	49.81	105.84	203.61	349.39	309.62	554664
304.44	580.52	311.16	640.07	52.31	112.79	205.98	352.53	309.63	694079
306.29	638.03	312.99	641.39	54.85	119.73	208.34	355.75	309.63	1192110
307.95	955.50	314.82	642.48	57.42	126.76	210.70	358.90	309.63	2235015
309.00	3654.50	316.64	644.08	60.02	133.68	213.04	362.11	309.63	2709567
309.39	15184	318.47	645.36	62.65	140.50	215.37	365.48	309.64	241313
309.51	38814	320.29	646.72	65.30	146.96	217.69	368.79	310.06	2586
309.56	77460	Series 3		67.99	153.43	220.00	372.16	311.36	640.15
309.58	135209	7.12	1.21	70.69	159.70	222.29	375.49	313.17	641.34
309.60	225510	8.37	2.26	73.41	165.86	224.58	378.96	314.99	642.52
309.61	389388	9.42	2.87	78.98	177.10	226.86	382.31	316.80	643.71
309.62	606765	10.76	4.20	81.73	182.67	229.13	385.54	318.61	645.03
309.62	860726	12.24	5.58	84.42	187.94	231.39	389.13	320.41	646.24
309.62	935781	14.03	8.80	87.05	192.91	233.64	392.62	322.22	647.71
309.63	1145634	15.74	11.39	89.60	197.59	235.88	396.22	324.02	649.15
309.63	1159154	17.66	14.97	92.08	201.98	238.11	399.73	325.82	650.70
309.63	1381878	19.76	19.68	94.51	206.27	240.33	403.02	Series 8	
309.63	1977671	21.92	24.70	96.89	210.30	242.54	406.33	327.31	652.12
309.63	2835136	24.19	30.66	99.22	213.98	244.74	409.80	328.75	653.38
309.64	1125440	26.57	37.12	Series 7		246.94	413.41	330.47	654.40
309.64	230966	29.04	44.28	102.20	218.84	249.12	416.95	332.45	655.96
309.81	7344	Series 4		104.94	223.23	251.30	420.72	334.43	657.79
310.89	638.50	7.54	1.65	107.73	227.49	253.47	424.21	336.42	659.90
312.70	640.80	9.38	2.91	110.61	231.73	255.63	428.04	338.40	661.28
314.51	642.12	10.88	4.09	113.49	235.71	257.78	431.78	340.38	663.18
316.32	643.55	12.68	5.98	116.38	239.83	259.92	435.60	342.37	664.66
318.12	644.70	14.52	8.84	119.27	243.78	262.05	439.33	344.35	666.56
319.92	646.05	16.32	12.16	122.18	247.71	264.18	443.27	346.34	668.31
321.72	647.37	18.29	16.20	125.09	251.61	266.29	447.25	348.32	669.95
323.51	648.62	20.44	21.10	128.00	255.60	268.40	451.35	350.31	671.97
325.31	650.06	22.66	26.65	130.91	259.45	270.50	455.48	352.30	673.88
Series 2		24.98	32.58	133.80	262.92	272.59	459.78	354.29	675.79
275.01	458.46	27.41	39.28	136.66	266.70	274.68	464.00	356.27	677.73
275.44	459.33	29.92	46.87	139.50	270.30	276.76	468.72	358.26	679.42
276.65	464.12	32.52	54.17	142.30	273.71	278.83	473.14	360.25	681.79
278.64	470.01	Series 5		145.07	277.12	280.89	477.84	362.25	683.73
280.63	475.40	6.69	0.88	147.82	280.46	282.94	482.87	364.24	685.39
282.61	480.97	8.98	2.73	150.54	283.75	284.99	488.11	366.23	687.09
284.59	486.57	11.12	4.22	153.24	286.98	287.02	493.07	368.22	689.04
286.58	492.28	12.69	5.89	155.92	290.13	289.04	498.80	370.21	691.34
288.56	497.93	14.53	8.76	158.58	293.35	291.06	504.52	372.21	693.07
290.54	503.27	16.37	12.27	161.22	296.43	293.06	510.68	374.20	695.38
292.52	509.67	18.35	16.20	163.84	299.61	295.05	517.77	376.19	697.52
294.50	516.45	20.49	21.01	166.44	302.77	297.03	525.07	378.19	699.11
296.48	523.55	22.72	26.46	169.02	305.90	299.00	533.27	380.18	700.99
298.46	531.45	25.05	32.45	171.58	308.98	300.96	543.97	382.18	703.08
300.43	541.41	27.46	39.30	174.13	312.15	302.89	559.16	384.17	705.00
302.37	555.51	29.97	46.62	176.67	315.23	304.80	585.33	386.17	707.62
304.29	579.44	32.57	54.04	179.18	318.34	306.64	658.99	388.16	709.42
306.16	636.23	Series 6		181.69	321.40	308.23	1118.89	390.16	711.43
307.86	911.56	32.43	54.02	184.18	324.45	309.15	5001	392.16	713.64
308.97	3214	33.76	57.86	186.65	327.55	309.44	20532	394.15	713.94
309.39	15113	35.59	63.49	189.11	330.69	309.54	47936	396.15	717.40
309.51	38232	37.93	70.54	191.56	333.79	309.58	116969	398.15	719.24

The maximum deviation of the experimental data from this fit is 0.2%.

Entropy at 298.15 K. Finke et al. (1954) fitted the available experimental entropy data at 298.15 K for the 14 alkanes ranging from C_5H_{12} to $C_{18}H_{38}$. They used a linear fit of the entropy against the number of carbon atoms. Messerly et al. (1967) applied a quadratic fit, which gave a smaller standard deviation. Although the compounds we measured have melting points higher than 298.15 K, the entropy of the liquid phase can be extrapolated to 298.15 K using a fit of the heat capacity data of the liquid. In Table 7, we compare the measured entropy values and the calculated with these fits. Both fits correspond well with our data. The quadratic fit differs by only 0.1% for $C_{19}H_{40}$ and 0.05% for $C_{20}H_{42}$. The larger difference of the quadratic fit from the data of Andon and Martin (1976) indicates that the quadratic fit cannot be extrapolated to $C_{26}H_{54}$.

Cooling Behavior. In Figures 3 and 4 a cooling curve for each compound is given. In the case of nonadecane, crystallization started at 304.80 K with no visible subcooling effect. This is remarkable, since the end melting point, which is the equilibrium temperature at a melted fraction (F) of 1, is 304.90 K. This is not exactly the same temperature as the triple point (305.00 K), which was determined by extrapolation to $1/F = 0$. During a cooling experiment, the outer part of the calorimeter vessel will be colder than the contents, since it is not an equilibrium process. The thermometer will show the temperature of the wall of the vessel, so the crystallization process actually

Table 4. Thermodynamic Properties at Selected Temperatures for *n*-Eicosane (M = 282.55 g.mol^{-1}, Φ_m° $\overset{\text{def}}{=}$ $\Delta_0^T S_m^{\circ} - \Delta_0^T H_m^{\circ}/T$)

T/K	$C_{p,m}^{\circ}$/ J·K^{-1}·mol^{-1}	ΔS_m°/ J·K^{-1}·mol^{-1}	ΔH_m°/ J·mol^{-1}	Φ_m°/ J·K^{-1}·mol^{-1}
10	3.20	1.07	8.0	0.270
15	9.69	3.59	39.8	0.939
20	20.22	7.76	113.4	2.089
25	32.57	13.56	244.4	3.778
30	46.68	20.75	442.7	5.990
35	61.69	29.06	713.4	8.681
40	76.92	38.29	1060	11.80
45	91.83	48.22	1482	15.29
50	106.39	58.65	1978	19.10
55	120.15	69.44	2544	23.18
60	133.62	80.48	3179	27.50
65	146.22	91.68	3879	32.00
70	158.12	102.96	4640	36.67
75	169.09	114.25	5459	41.46
80	179.17	125.48	6330	46.36
85	189.04	136.65	7251	51.35
90	198.31	147.72	8219	56.39
95	207.12	158.68	9233	61.49
100	215.24	169.51	10289	66.62
105	223.33	180.21	11385	71.77
110	230.86	190.77	12521	76.94
120	244.77	211.46	14900	87.30
130	258.27	231.59	17415	97.62
140	270.92	251.19	20061	107.90
150	283.09	270.29	22831	118.09
160	295.00	288.95	25722	128.19
170	307.07	307.19	28732	138.18
180	319.34	325.09	31864	148.07
190	331.82	342.69	35119	157.85
200	344.68	360.03	38501	167.53
210	357.97	377.17	42014	177.10
220	372.16	394.14	45663	186.58
230	386.90	411.01	49459	195.97
240	402.53	427.81	53407	205.28
250	418.46	444.56	57510	214.52
260	435.74	461.30	61780	223.69
270	454.49	478.09	66229	232.80
280	475.77	495.00	70878	241.86
290	501.52	512.13	75760	250.89
300[a]	528.24	529.58	80907	259.89
309.65[a,b]	556.19	546.73	86137	268.56
309.65[c]	638.78	772.34	155996	268.56
310	639.02	773.08	156219	269.15
320	645.19	793.44	162645	285.17
330	654.11	813.45	169135	300.92
340	662.67	833.11	175720	316.29
350	671.74	852.45	182398	331.31
360	681.23	871.51	189170	346.04
370	691.03	890.30	196035	360.48
380	701.02	908.85	202994	374.65
390	711.10	927.19	210047	388.61

[a] Extrapolation from the solid; temperature range used 230−295 K. [b] Solid [c] Liquid

Table 5. Measured Enthalpies of Transition and Melting of *n*-Nonadecane

series	$\Delta H_{trans} + \Delta H_{fus}$/J·mol^{-1}
1	62672
2	62652
7	62653
mean value and estimated error	62659 ± 20

starts at a temperature even higher than 304.80 K. We conclude that this compound crystallizes at or very near its melting point. To determine if the material of the vessel influenced the start of the crystallization, we did some measurements in a Hart calorimeter. This is a commercial microcalorimeter with three measuring vessels having volumes of about 1 cm^3. A Teflon holder was placed in one of the stainless steel vessels. Crystallization started at
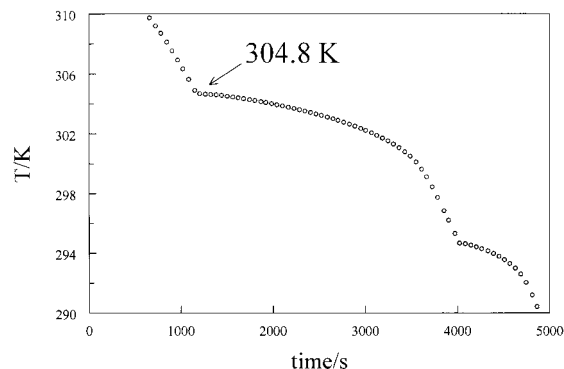
Figure 3. Cooling curve of *n*-nonadecane; crystallization starts within 0.1 K of the final melting point.
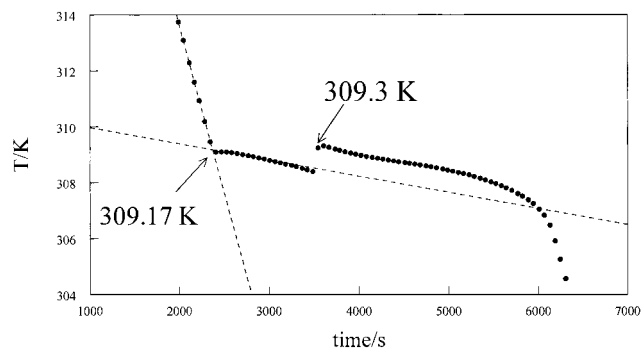
Figure 4. Cooling curve of *n*-eicosane. The compound crystallizes in a metastable state; when about 40% is crystallized, it transforms to the stable crystal form.

Table 6. Measured Enthalpies of Fusion of *n*-Eicosane

series	triple point/K	enthalpy of fusion/J·mol^{-1}	purity/%
1	309.65	69876	99.91
2	309.65	70013	99.90
7	309.65	69877	99.91
mean value	309.65	69922 ± 100	99.91

Table 7. Measured and Calculated Entropy Values at 298.15 K

	$\Delta S(C_{19}H_{40})$/ J·K^{-1}·mol^{-1}	$\Delta S(C_{20}H_{42})$/ J·K^{-1}·mol^{-1}	$\Delta S(C_{26}H_{54})$/ J·K^{-1}·mol^{-1}
this work	715.9	748.1	945 (Andon and Martin, 1976)
Finke (linear fit)	716.7	749.0	943
Messerly (quadratic fit)	716.4	748.5	940.5

exactly the same temperature both with and without the Teflon holder at a cooling rate of 1 K·min^{-1}. This behavior makes this alkane an ideal temperature calibration compound for cooling experiments in a differential scanning calorimeter.

Eicosane crystallizes first in a metastable phase. When about 40% is crystallized, a sudden transition to the stable phase takes place. Crystallization of the metastable phase started at 309.17 K; no subcooling was observed. Experiments in the Teflon holder mentioned before also showed no influence of the material of the wall of the vessel.

Literature Cited

Andon, R. J. L.; Martin, J. F. Thermodynamic Properties of Hexacosane. *J.Chem. Thermodyn.* **1976**, *8*, 1159−1166.

Aston, J. G.; Messerly, G. H. The Heat Capacity and Entropy, Heats of Fusion and Vaporization and the Vapor Pressures of *n*-Butane. *J. Am. Chem. Soc.* **1940**, *62*, 1917−1923.

Atkinson, C. M. L.; Larkin, J. A.; Richardson, M. J. Enthalpy Changes in Molten *n*-Alkanes and Polyethylene. *J. Chem. Thermodyn.* **1969**, *1*, 435−440.

Barbillon, P.; Schuffenecker, L.; Dellacherie, J.; Balesdent, D.; Dirant, M. Variation d'Enthalpie Subie de 260 K à 340 K par les n-Paraffines, Comprises entre l'Octodécane (n-C$_{18}$) et l'Hexocosane (n-C$_{26}$). *J. Chim. Phys.* **1991**, *88*, 91−113.

Claudy. P.; Létoffe, J. M. Transition de Phase dans les n-Alcanes Pairs C$_n$H$_{2n+2}$ n=16−28. *22-èmes Journées de Calorimétrie et d'Analyse Thermique* **1991**, 281−290.

Finke, H. L.; Gross, M. E.; Waddington, G.; Huffman, H. M. Low-Temperature Thermal Data for the Nine Normal Paraffin Hydrocarbons from Octane to Hexadecane. *J. Am. Chem. Soc.* **1954**, *76*, 333−341.

Huffman, H. M.; Parks, G. S.; Barmore, M. Thermal Data on Organic Compounds. X. Further Studies on the Heat Capacities, Entropies and Free Energies of Hydrocarbons. *J. Am. Chem. Soc.* **1937**, *53*, 3876−3888.

Kemp, J. D.; Egan, C. J. Hindered Rotation of the Methyl Groups in Propane. The Heat Capacity, Vapor Pressures, Heats of Fusion and Vaporization of Propane. Entropy and Density of the Gas. *J. Am. Chem. Soc.* **1938**, *60*, 1521−1525.

Messerly, J. F.; Guthrie, G. B.; Todd, S.; Finke, H. L. Low-Temperature Thermal Data for *n*-Pentane, *n*-Heptadecane, and *n*-Octadecane. *J. Chem. Eng. Data* **1967**, *12*, 338−346.

Mondieig, D.; Espeau, P.; Robles, L.; Haget, Y.; Oonk, H. A. J.; Cuevas-Diarte, M. A. Mixed Crystals of *n*-Alkane Pairs. A Global View of the Thermodynamic Melting Properties. *J. Chem. Soc., Faraday Trans.* **1997**, *93*, 3343−3346.

Oonk, H. A. J.; Mondieig, D.; Haget, Y.; Cuevas-Diarte, M. A. Perfect Families of Mixed Crystals: The Rotator I *N*-Alkane Case. *J. Chem. Phys.* **1998**, *108*, 715−722.

Parks, G. S.; Huffman, H. M.; Thomas, S. B. Thermal Data on Organic Compounds. VI. The Heat Capacities, Entropies and Free Energies of Some Saturated, non-Benzenoid Hydrocarbons. *J. Am. Chem. Soc.* **1930**, *52*, 1032−1041.

Parks, G. S.; Shomate, C. H.; Kennedy, W. D.; Crawford, B. L. The Entropies of *n*-Butane and Isobutane, with Some Heat Capacity Data for Isobutane. *J. Chem. Phys.* **1937**, *5*, 359−363.

Parks, G. S.; Moore, G. E.; Renquist, M. L.; Naylor, B. F.; McLaine, L. A.; Fujii, P. S.; Hatton, J. A. Thermal Data on Organic Compounds. XXV. Some Heat Capacity, Entropy and Free Energy Data for Nine Hydrocarbons of High Molecular Weight. *J. Am. Chem. Soc.* **1949**, *71*, 3386−3389.

Preston-Thomas, H. The International Temperature Scale of 1990 (ITS-90). *Metrologia* **1990**, *27*, 3−10.

Schaerer, A. A.; Busso, C. J.; Smith, A. E.; Skinner, L. B. Properties of Pure Normal Alkanes in the C$_{17}$ to C$_{36}$ Range. *J. Am. Chem. Soc.* **1955**, *77*, 2017−2019.

Stull, D. R. A Semi-Micro Calorimeter for Measuring Heat Capacities at Low Temperatures. *J. Am. Chem. Soc.* **1937**, *59*, 2726−2733.

van Miltenburg, J. C.; van der Berg, G. J. K.; van Bommel, M. J. Construction of an Adiabatic Calorimeter. Measurement of the Molar Heat Capacity of Synthetic Sapphire and of *n*-Heptane. *J. Chem. Thermodyn.* **1987**, *19*, 1129−1137.

Witt, R. K.; Kemp, J. D. The Heat Capacity of Ethane from 15 K to the Boiling Point. The Heat of Fusion and the Heat of Vaporisation. *J. Am. Chem. Soc.* **1937**, *59*, 273−279.